MIHAEL MACHADO DE SOUZA

MODELAGEM COMPUTACIONAL DO COMPLEXO ESTUARINO DE PARANAGUÁ SOB A INFLUÊNCIA DE ONDAS, MARÉS E DESCARGA FLUVIAL

Pontal do Paraná

Março de 2015

MIHAEL MACHADO DE SOUZA

MODELAGEM COMPUTACIONAL DO COMPLEXO ESTUARINO DE PARANAGUÁ SOB A INFLUÊNCIA DE ONDAS, MARÉS E DESCARGA FLUVIAL

Dissertação apresentada ao Curso de Pós-Graduação em Sistemas Costeiros e Oceânicos, Universidade Federal do Paraná, como requisito parcial a obtenção do grau de Mestre.

Orientador: Dr. Carlos Alessandre Domingos Lentini

Co-Orientador: Dr. Mauricio Almeida Noernberg

Pontal do Paraná

Março de 2015

CATALOGAÇÃO NA FONTE:
UFPR / SIBI - Biblioteca do Centro de Estudos do Mar
Liliam Maria Orquiza - CRB-9/712

SOUZA, Mihael Machado de
S729m Modelagem computacional do Complexo Estuarino de Paranaguá sob a influência de ondas, marés e descarga fluvial. / Mihael Machado de Souza. – Pontal do Paraná, 2015.
41 f.; 29 cm.

Orientador: Prof. Dr. Carlos Alessandre Domingos Lentini.
Co-Orientador: Dr. Mauricio Almeida Noernberg.

Dissertação (Mestrado) – Programa de Pós-Graduação em Sistemas Costeiros e Oceânicos, Centro de Estudos do Mar, Setor de Ciências da Terra, Universidade Federal do Paraná.

1. Delft3D. 2. Complexo Estuarino de Paranaguá. 3. Circulação Residual. 4. Fluxos de Sal. 5. Ciclo Sizígia-Quadratura. I.Título. II. Lentini, Carlos Alessandre Domingos. III. Noernberg, Maurício Almeida. IV. Universidade Federal do Paraná.

CDD 551.47

PGSISCO
CURSO DE PÓS-GRADUAÇÃO EM SISTEMAS COSTEIROS E OCEÂNICOS
Centro de Estudos do Mar - Setor Ciências da Terra - UFPR
Avn. Beira-mar, s/nº - Pontal do Sul - Pontal do Paraná - Paraná - Brasil
Tel. (41) 3511-8644 - Fax (41) 3511-8648 - www.cem.ufpr.br - E-mail: pgsisco@ufpr.br

TERMO DE APROVAÇÃO

Mihael Machado de Souza

Modelagem Computacional do Complexo Estuarino de Paranaguá sob a influência de Ondas, Marés e Descarga Fluvial

Dissertação aprovada como requisito parcial para a obtenção do grau de Mestre(a) em Sistemas Costeiros e Oceânicos, da Universidade Federal do Paraná, pela Comissão formada pelos professores:

Dr. Carlos Alessandre Domingos Lentini (UFBA)
Orientador e Presidente

Dr. Eduardo Marone (UFPR/CEM)
Membro Examinador

Dra. Cynara de Lourdes da Nóbrega Cunha (UFPR)
Membro Examinador

Dr. Carlos Augusto França Schettini (UFPE)
Membro Examinador

Pontal do Paraná, 24/03/2015.

“Lembre-se que as pessoas podem tirar
tudo de você, menos o seu
conhecimento.”
Albert Einstein

AGRADECIMENTOS

Antes de tudo, gostaria de agradecer aos meus pais que sempre me estimularam e incentivaram a dar meu máximo em qualquer coisa que eu faça. Independente das minhas decisões eles sempre estiveram do meu lado, e isso tem um significado enorme para mim. Vocês são meu exemplo de vida, pessoal e profissional. Obrigado e amo muito vocês.

Aos meus orientadores, Lentini e Maurício, um agradecimento especial pela paciência em alguns momentos, e pelas discussões intrigantes a cerca dos resultados deste trabalho. Aprendi muito ao longo destes dois anos, e é um conhecimento que vai me ajudar nas etapas que vêm pela frente. Ao Lentini, em especial, pela oportunidade de me aventurar em uma área nova e me dar toda a base necessária para realizar esta dissertação.

À Ana, me faltam palavras para colocar no papel todo o agradecimento que tenho por ti. Já são sete anos juntos, com tudo que um relacionamento inclui. A única coisa que posso dizer é que eu aprendi muito contigo e tenho um orgulho enorme da pessoa e cientista que você é. Te amo minha *petit*.

Aos amigos, agradeço pelos churrascos, cervejas e conversas ao longo dos anos. Sempre existia um ouvido amigo para ajudar nos momentos de dúvida, e pra dar boas risadas quando estávamos todos por baixo. Ao GRR2008, tanto aos que ficaram quanto aos que já estão fazendo suas vidas mundo afora, muito obrigado pela amizade de todos.

Um grande agradecimento a todos os professores e colegas de profissão que disponibilizaram dados para a implementação do modelo numérico utilizado neste trabalho – Dr. César de Castro Martins, Dra. Eunice da Costa Machado, MSc. Bruno Libardoni, MSc. Marília Rocha, MSc. Rafaela Zem; ao convênio APPA – CEM pelos dados de maré; e ao Edson Nagashima, do Instituto das Águas do Paraná, pelos dados de vazão diária dos rios Cachoeira e Nhundiaquara. Sem estas informações este trabalho não seria possível.

Por fim, a CAPES pela bolsa de estudos dos últimos dois anos, e a UFPR e PGSISCO, em especial aos professores, pela oportunidade de me aperfeiçoar na ciência que escolhi como meu futuro. Muito obrigado.

SUMÁRIO

RESUMO GERAL 2

HYDRODYNAMICS AND SALT TRANSPORT IN A SUBTROPICAL ESTUARY UNDER VARYING WAVES AND FRESHWATER DISCHARGE CONDITIONS 5

1. INTRODUCTION 7

2. METHODS 8

2.1 Study Site *8*

2.2 Model setup *11*

2.3 Boundary Conditions *12*

2.4 Evaluated scenarios *13*

3. RESULTS 17

3.1 Model verification *17*

3.2 Effects of a variable boundary forcing in hydrodynamics and stratification *19*

3.3 Consequences on the advective salt flux *25*

4. DISCUSSION AND CONCLUSIONS 27

REFERENCES 31

RESUMO GERAL

Estuários estão sujeitos a variações nas suas forçantes externas em diferentes escalas de tempo, de algumas horas até a escala de anos. O fluxo de água doce (Q_f) é considerado uma das mais importantes fontes de variabilidade, pois influencia o fluxo residual de água; enquanto que a ação de ondas no estuário depende da batimetria em sua desembocadura e atua principalmente na turbulência e na mistura vertical. Estudar esta variabilidade, e a interação destas forçantes, permite entender o padrão geral de circulação dentro do sistema estuarino e o transporte de substâncias dissolvidas, o que permite a criação de estratégias para mitigar danos provocados nestes ambientes em decorrência da ação antrópica. Este trabalho tem como objetivo investigar o impacto do aumento da vazão de água doce e da ação de um campo de ondas realístico na hidrodinâmica e no transporte de sal de um estuário de micromaré subtropical, o Complexo Estuarino de Paranaguá (CEP), considerando a escala de tempo de modulação sizígia-quadratura.

O *Delft-3D* foi utilizado para implementar um modelo baroclínico do Complexo Estuarino de Paranaguá, e os resultados foram extraídos a partir de dois cenários simulados. Este modelo apresenta resolução espacial variável, entre 25 e 300 metros dentro da área de interesse, com 14 camadas verticais do tipo sigma. A rugosidade de fundo foi calculada em função da batimetria e dos sedimentos, e os coeficientes de viscosidade e difusividade horizontais foram obtidos do trabalho de Mayerle et al. (2015). Na vertical, as simulações utilizaram um modelo de fechamento turbulento do tipo k-Ɛ (WL|DelftHydraulics, 2006). A implementação utilizada foi validade em relação às marés, velocidade das correntes, características do trem de ondas, e ao gradiente longitudinal de salinidade; utilizando dados disponibilizados pela parceria entre o CEM e a Paranaguá Pilots, dados do Laboratório de Geoquímica e Poluição Marinha (LaGPoM), dados de uma bóia meteo-oceanográfica fundeada no escopo do projeto do INCT-Mar COI, e a literatura disponível na região (Nemes and Marone, 2013; Noernberg, 2001). O modelo apresentou uma boa resposta para todas as propriedades analisadas, com o menor valor encontrado do índice de concordância (Willmott et al., 2012) sendo para a salinidade (d_r = 0,73). Referente às correntes, o modelo foi capaz de reproduzir bem a componente longitudinal da circulação (d_r = 0,80), porém a componente transversal não

apresentou um bom resultado. Isto está possivelmente relacionado ao modelo não conseguir resolver bem os fluxos advindos do Canal da Cotinga, já que a resolução espacial do modelo nesta região é de apenas algumas células, e a área apresenta uma batimetria complexa.

Inicialmente, uma simulação de seis meses compreendendo a variabilidade sazonal da descarga fluvial foi realizada, seguida de uma simulação mais curta, compreendendo apenas o período de maior descarga de água doce combinada ao campo medido de ondas. Para cada simulação, um período de *spin-up* de dois meses foi utilizado para garantir a estabilidade dos campos de salinidade antes dos cenários de interesse. Resultados mostraram que a as marés foram dominantes em determinar a hidrodinâmica da Baía de Paranaguá, com valores do número de Richardson estuarino indicando uma influência 2x maior da maré mesmo em períodos de alta vazão na porção mais a montante do sistema. As ondas atuaram principalmente como uma cerca de energia, reduzindo a magnitude da circulação residual, e afetaram diretamente apenas a estratificação na zona mais externa do estuário. De maneira geral, os bancos arenosos na plataforma interna rasa foram muito eficientes em mitigar a energia das ondas e proteger o estuário em eventos de *swell*. No tocante aos padrões hidrodinâmicos resultantes, uma circulação residual bidirecional foi verificada tanto na escala vertical quanto horizontal ao longo do gradiente salino do estuário, e o aumento na descarga de água doce não provocou alterações nestes padrões. A descarga de água doce na porção superficial da coluna d'água dominou os processos advectivos do transporte de sal, enquanto a circulação gravitacional e a correlação de maré foram os principais mecanismos de dispersão de sal ao longo deste sistema, o último indicando uma grande importância dos baixios e áreas rasas na hidrodinâmica da Baía de Paranaguá. Dois sistemas de classificação foram testados para o ambiente. O clássico sistema de Hansen and Rattray (1965) classifica o estuário como do tipo parcialmente misturado, e já havia sido utilizado para o CEP (Lana et al., 2001). Usando o sistema de classificação proposto por Geyer and MacCready (2014), o estuário foi caracterizado dentro do regime SIPS, o que indica uma estratificação periódica da coluna d`água ao longo do ciclo de mare. Está classificação é suportada pelos valores obtidos para o número de Simpson, que ficaram no intervalo entre 0,2 e 0,8. Do ponto de vista dinâmico, isso indica um padrão cíclico de destruição e reconstrução da estratificação vertical ao longo do ciclo de maré através da turbulência gerada pela propagação da onda de maré. O resultado

deste processo é um estuário mais bem misturado durante as enchentes, e parcialmente misturado durante as vazantes.

Revista pretendida: Continental Shelf Research

Qualis: B1 em Biodiversidade

Fator de Impacto: 1,892

HYDRODYNAMICS AND SALT TRANSPORT IN A SUBTROPICAL ESTUARY UNDER VARYING WAVES AND FRESHWATER DISCHARGE CONDITIONS

SOUZA, M. M. de[1,3,5]; LENTINI, C. A. D.[2,3]; NOERNBERG, M. A.[1]; GONÇALVES, J. E.[4]

[1] Pós-Graduação em Sistemas Costeiros e Oceânicos (PGSISCO) - Centro de Estudos do Mar, Universidade Federal do Paraná – CEM/UFPR. Av. Beira-mar, s/n, Balneário Pontal do Sul, Pontal do Paraná, PR, Brazil.

[2] Instituto de Física – Departamento de Física da Terra e do Meio Ambiente, Universidade Federal da Bahia – UFBA.

[3] GOAT - Grupo de Oceanografia Tropical - http://www.goat.fis.ufba.br

[4] Instituto Tecnológico SIMEPAR. Centro Politécnico da UFPR, Curitiba, PR, Brazil.

[5] E-mail: mihaelsouza@gmail.com

RESUMO

Estuários estão sujeitos a variações nas suas forçantes externas em diferentes escalas de tempo. O fluxo de água doce (Q_f) é considerado uma das mais importantes fontes de variabilidade, enquanto que a ação de ondas no estuário depende da batimetria em sua desembocadura. Estudar esta variabilidade permite entender o padrão geral de circulação dentro do sistema estuarino e o transporte de substâncias dissolvidas. Este trabalho tem como objetivo investigar o impacto do aumento de Q_f e da ação de um campo de ondas realístico na hidrodinâmica e no transporte de sal de um estuário de micromaré subtropical, considerando a escala de tempo de modulação sizígia-quadratura. O *Delft-3D* foi utilizado para implementar um modelo baroclínico do Complexo Estuarino de Paranaguá, e dois cenários foram simulados. Inicialmente, uma simulação de seis meses compreendendo a variabilidade sazonal da descarga fluvial foi realizada, seguida de uma simulação do período de maior descarga doce

combinada ao campo medido de ondas. Resultados mostraram que a as marés foram dominantes em determinar a hidrodinâmica da Baía de Paranaguá, com Q_f e as ondas apresentando poucos efeitos. As ondas atuaram como uma cerca de energia reduzindo a magnitude da circulação residual, e afetaram diretamente apenas a estratificação na zona mais externa do estuário. Uma circulação residual bidirecional foi verificada tanto na escala vertical quanto horizontal ao longo do gradiente salino do estuário, com a descarga de água doce na porção superficial da coluna d'água dominando os processos advectivos do transporte de sal. A circulação gravitacional e a correlação de maré foram os principais mecanismos de dispersão de sal ao longo deste sistema, o último indicando uma grande importância dos baixios e áreas rasas na hidrodinâmica da Baía de Paranaguá. Usando o sistema de classificação proposto por Geyer and MacCready (2014), o estuário foi caracterizado dentro do regime SIPS, o que indica uma estratificação periódica da coluna d`água ao longo do ciclo de mare.

Palavras-chave: Delft3D, Complexo Estuarino de Paranaguá, Circulação Residual, Fluxos de Sal, *Ciclo Sizígia-Quadratura.*

ABSTRACT

Estuaries are subject to variations in forcing mechanism across different time scales. Freshwater flow (Q_f) is considered one of the most important sources of variability, while wave action is dependent on the morphological setting at the estuary's mouth. Studying this variability is important to understand the overall estuarine dynamics and the transport of dissolved constituents. This work aims to investigate the impact of a rising freshwater discharge and a realistic wave field to the hydrodynamics and salt transport of a microtidal subtropical estuary, considering the fortnightly time scales. Delft3D was used to implement a 3-D baroclinic model of the Paranaguá Estuarine Complex, and two scenarios were devised. A six-month simulation comprehending a complete seasonal variation of freshwater flow as performed, and then the highest freshwater discharge scenario was re-simulated to account for the wave field. Results showed that tides dominated the shaping of the hydrodynamics in Paranaguá Bay, with Q_f and waves contributing only slightly. Waves acted as an energy fence reducing the overall magnitude of the residual circulation in the estuary, but only directly affected mixing inside the

outer zones. A residual two-layer circulation on the vertical and horizontal scales was found along the salinity gradient of the estuary, with the advection of salt through the surface freshwater flow dominating the advective salt fluxes. As dispersion mechanisms, gravitational circulation and tidal correlation were dominant, the latter indicating a high importance of the shallow areas to the overall bay dynamics. Using Geyer and MacCready (2014) classification, the Paranaguá Bay was characterized under the SIPS regime, indicating that periodic stratification of the water column can be expected along the tidal cycle.

Keywords: Delft3D, Paranaguá Estuarine Complex, Residual Circulation, Salt Fluxes, *Fortnightly Cycle.*

1. INTRODUCTION

Estuaries are transition environments between riverine systems and the adjoining costal ocean in which the complex nonlinear interaction of tides, currents, salt, water and sediment occur. It has a restricted connection to the ocean that remains open at least intermittently, and can be subdivided into three subregions: a tidal river zone, a mixing zone, and a nearshore turbid zone (Kjerfve, 1989). A wide range of processes and mechanisms influences the shape and evolution of this region, from bathymetry and bed morphology to tidal regime and wave climate. The monitoring of all these conditions is labor-intensive and expensive. The use of models are considered essential for case studies, providing a thorough investigation of forcing mechanisms as well as fast predictions and forecasts (Hu et al., 2009; Lesser et al., 2004), which in turn allows a synoptic view of the study site and provides valuable information on governing flows and transport pathways (Elias and Hansen, 2013).

In this environment, rivers act as a positive buoyancy forcing that alters the fluid density from the adjoining ocean, creating a bidirectional circulation known as the exchange flow or the estuarine circulation (Geyer and MacCready, 2014), while the tidal forces are generally considered dominant in generating turbulent mixing (MacCready, 2011; Miranda et al., 2002). Besides the classical gravitational circulation pattern of an up-estuary bottom flow and a down-estuary surface flow, Burchard et al. (2011) showed that tidal straining (Simpson et al., 1990) can have an equal contribution to the residual circulation in the presence of lateral advective

mechanisms, such as the ones described by Lerczak and Geyer (2004). Waves, on the other hand, have been shown to present a non-linear interaction with tidal currents. Luo et al. (2013) studied three estuaries with different morphological settings at Liverpool Bay (Mersey, Dee and Ribble), and showed that on systems with large inlets waves can have an effect on circulation, but Bolaños et al. (2014) focused on the effect of this interaction along the tidal cycle in the Dee estuary, and found that waves contribute only marginally to overall current velocities. In this sense, analyzing the dynamic processes leading to residual circulation patterns in estuaries are important to gain knowledge of the relevant salt fluxes (MacCready, 2011).

The two most important sources of variability to estuarine dynamics are considered the spring-neap modulation of tidal forcing and the variations in freshwater flow, although wind-forcing and sea-level variations can also cause changes in the estuarine regime (MacCready and Geyer, 2010). Previous studies for the Paranaguá Estuarine Complex tried to considered both sources of variability, the spring-neap modulation and changes in freshwater regime, by means of measurements during one or two tidal cycles at different seasons (Mantovanelli et al., 2004; Marone et al., 2007; Noernberg et al., 2007). The problem with this approach is that hydrographic campaigns are generally planned during the highest springs and lowest neaps in order to account for the largest tidal variability in the space domain. However, Lerczak et al. (2006) stress out that this approach will give limited information about the variations in the amplitude of downgradient salt fluxes and dominant dispersion mechanisms under different forcing conditions. Therefore, our goal is to evaluate the effects of different freshwater regimes to the residual circulation pattern and salt fluxes of a well-mixed to partially-mixed subtropical estuary, considering the complete energy gradient of a fortnightly cycle, as well as the impact of a realistic wave field on the CEP's hydrodynamic behavior.

2. METHODS

2.1 Study Site

The Paranaguá Estuarine Complex (PEC – Fig. 1B) is located in the northern coast of the Paraná state, Brazil, and presents a semi-diurnal tidal regime with amplitudes just under 2 m at the estuarine inlets (Marone and Jamiyanaa, 1997). According to these authors, the PEC can be classified as a tide-dominated system presenting an asymmetrical tidal cycle with longer

floods and shorter ebbs and double high and low water effects. Based on hydrological and morphological characteristics, Noernberg et al. (2006) divided the PEC into five sectors, three of which comprises the E-W axis of this system and are the focus of this study: 1 – a mixture zone (MZ), the Paranaguá bay (PB), and the Antonina bay (AB) (Fig. 1C). On the other hand, the other two sectors, the Laranjeiras and Pinheiros bays, which comprise the N-S axis of this system, are not the scope of this manuscript. The combination of the three sectors in the E-W axis will be referred here as the Paranaguá Bay. When necessary, these three sectors will be addressed separately and accordingly to the aforementioned acronyms.

Marone et al. (2005) described the Paranaguá Bay as having a volume of 1.8×10^9 m^3 and a surface area of 330 km^2, with a mean depth of 5.4 m and maximum depth of 33 m, and Noernberg et al. (2006) estimated a drainage density of 1.12 rivers/km². The area presents ebb-tidal deltas at both inlets with the occurrence of a semi flood-tidal delta at the southern inlet (Angulo, 1999). Through this inlet there is also a navigational channel that grants access to two different ports in the area, and it needs to be periodically dredged to maintain navigational depths (Soares and Lamour, 2008).

The typical horizontal salinity gradient ranges from 12 – 29 (austral summer) to 20 – 34 (austral winter) depending on freshwater input, with an approximated mean value up to 200 $m^3.s^{-1}$ (Lana et al., 2001; Marone et al., 2005) and contributed mainly by two rivers, the Cachoeira and Nhundiaquara rivers (Fig. 1B). Mizerkowski et al. (2012) evaluated, among other variables, the termohaline stratification of Paranaguá Bay through six longitudinal transects. They found that, at the PB sector, bottom salinities were constantly higher than surface values, and the AB sector was dominated by river discharge. These authors found horizontal salinity gradients similar to the ones reported by Marone et al. (2005). On the other hand, spatial differences in temperature were only marginal, with average values of 20 – 21ºC during the dry season (June – August) and 25 – 26ºC during the rainy season (November – February).

Regarding the Paranaguá Bay hydrodynamics, tidal currents tend to follow the dredged-in navigational channel (Noernberg et al., 2007) and present stronger ebb currents than flood currents throughout the water column. According to Mantovanelli et al. (2004) ebb currents can be up to 48% stronger than flood currents during spring tides. Few studies have been conducted regarding wave action in this region (Lana et al., 2001; Martins et al., 2004; Nemes

and Marone, 2013; Noernberg et al., 2007). Lana et al. (2001) reported waves inside the inlets to be 0.5 m high, with periods between 3 and 7 seconds, and preferentially from the SE quadrant. Noernberg et al. (2007) postulated that the turbulence generated by these waves may have an effect on amplifying bed load sediment transport and promote the navigational channel silting, based on a mooring data located over the inner shelf. Lastly, Nemes and Marone (2013) analyzed one year of wave data records from two buoys located at the inner shelf's 30 and 18 meters isobaths (25º 41`S e 48º 21`W and 25º 44`S e 48º 20`W, respectively), and characterized the wave climate for the region. They found out that, although at the 30 meters isobaths the wave spectra presents a bimodal distribution it can be represented by a monochromatic wave as it approaches the coast. They also reported some extreme events, which presented wave heights of over 4 m at the shallower buoy.

Bottom sediments are composed of a mixture of sand and muds throughout the estuary. The Cachoeira and Nhundiaquara river mouths at the AB sector are composed mainly of medium to coarse sand, grading until medium to fine silt at the PB sector, and then from fine to very fine sand at the inlets of the estuary, in the MZ sector. At the MZ sector, grains are well to very-well sorted, with organic and carbonate contents of less than 5%, and less than 10% of muds in the composition. At the PB and AB sector grains are generally poorly sorted, with variable carbonate percentages (5 – 20%) and organic contents of up to 35% (Lamour et al., 2004).

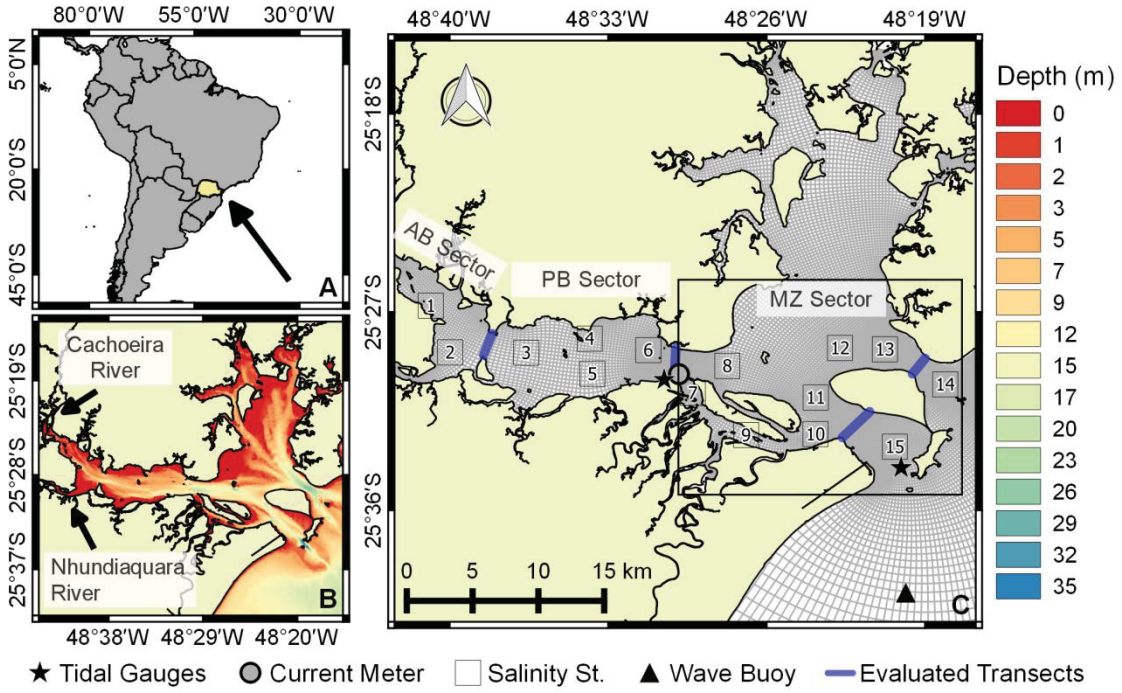

Figure 1 – The Paranaguá Estuarine Complex, with the model domain (C), the local bathymetry (B) and the available datasets for validation (C). Three sectors are defined: mixture zone (MZ), the Paranaguá bay (PB), and the Antonina bay (AB). The bathymetry is defined through the color scale, and the sectors corresponds to the definitions of Noernberg et al. (2006) for the area. The location of all available datasets is shown in symbols, as well as the location of the evaluated transects along the Paranaguá Bay (blue transects). Numbers on the squares indicate the position of salinity stations referenced on validation (fig. 4).

2.2 Model setup

Delft3D resolves the Reynolds-averaged Navier-Stokes and continuity equations for incompressible fluids in shallow waters, considering the Boussinesq approximation. For details on the equation system the reader is referred to the work of Lesser et al. (2004). A curvilinear grid was fit to the Paranaguá Estuarine Complex (Fig. 1B), with a horizontal resolution between 25 and 300 m and a total of 20392 grid points. A second modeling domain (not shown) comprising the inner continental shelf, from the 60 meters isobaths to the shore, was used solely to propagate waves and create boundary conditions for the estuarine domain. In the vertical, fourteen sigma layers were used, with increased resolution at the bottom and surface of the modeling domain; a 50% ratio between adjacent layers was respected (WL|DelftHydraulics, 2006). The time step adopted was of 60 seconds to ensure model stability, with results recorded

hourly. Wave fields were updated every two hours in the coupled simulation due to hardware restrictions, and SWAN (Simulating Waves Nearshore - Booji et al., 1999) ran a third-generation stationary mode considering the processes of depth-inducing breaking, whitecapping, refraction and frequency shift activated under default schemes. An accuracy of 99% of wet grid points was enforced to improve the generated wave field for the estuarine domain.

Bathymetry was compiled from a number of sources, comprising nautical charts and eco-soundings of the navigational channel and some sectors of the Laranjeiras Bay. A spatially variable bottom roughness was used, considering both the bathymetry and bottom sediments, and calculated through the White-Colebrook formula (WL|DelftHydraulics, 2006). Horizontal viscosity and diffusivity were obtained from the work of Mayerle et al. (2015), and verified during validation of the salinity gradients. For the definition of the vertical viscosity and diffusivity, the k-epsilon turbulence closure model was used. A constant temperature of 23ºC was enforced in every scenario, based on the findings of Mizerkowski et al. (2012).

2.3 Boundary Conditions

Water level data from a tidal gauge at the southern inlet of Paranaguá Bay (Fig. 1C) was made available, with records from 2006 – 2013. This data comes from a partnership between the Center for Marine Studies (CEM – UFPR) and the Paranaguá Pilots Company, and was used to calculate the tidal harmonics from which reconstructed tidal elevations for the desired modeling scenarios were performed. A fixed salinity of 33 was used as ocean boundary, extrapolated from the results of an ocean buoy recordings starting from 2013 (Fig. 1C).

Daily freshwater discharge values are available for five rivers inside the PEC from the Paraná's Water Institute (ÁguasParaná – Instituto das Águas do Paraná): Cachoeira, Nhundiaquara and Sagrado at the AB sector; and Tagaçaba and Guaraqueçaba at the N-S axis. These five rivers comprise only a fraction of the total drainage basin surrounding the PEC (Fig. 2). In order to have a better approximation to the total freshwater discharge in the area, a proportionality coefficient was applied (Miranda et al., 2012): $Q_t = Q_r * (A_t / A_r)$; where Q is the freshwater discharge, A is the drainage surface area, the subscript t refers to the whole basin, and subscript r refers to the nearest available riverine dataset. This relation gives at least an

approximation on the expected freshwater flows to the PEC, while maintaining the temporal variability captured from the available data. Data from the Cachoeira River, basin IV, was not used to estimate neighboring areas due to this discharge being controlled by a dam implemented along the river, so data from the Tagaçaba River was used instead for basins V and VI and Sagrado River dataset was used for basins II and I. All river boundaries were forced with a zero salinity condition.

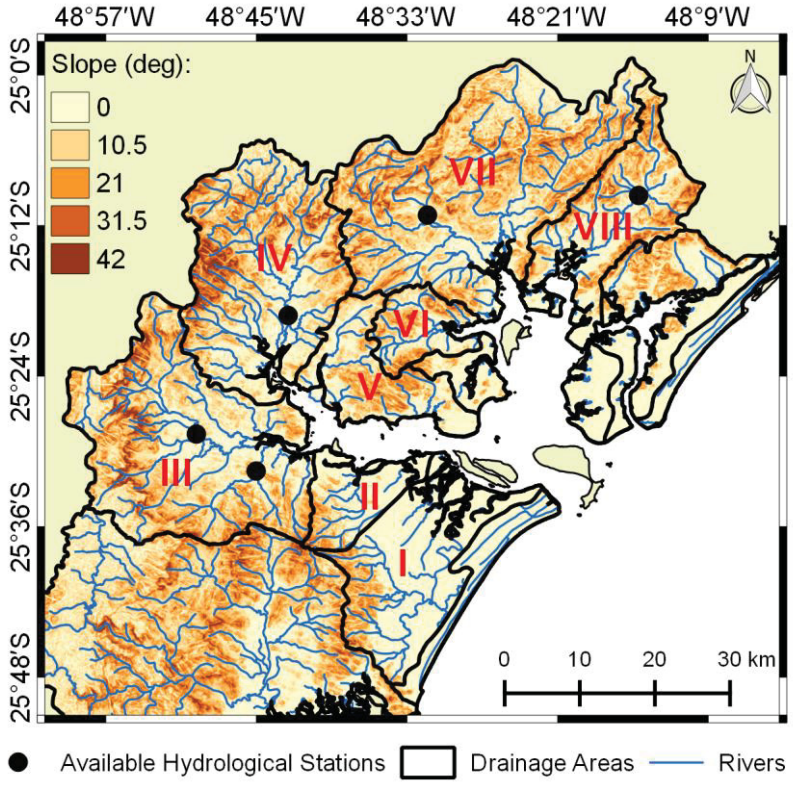

Figure 2 – Drainage areas (I-VIII) of The Paranaguá Estuarine Complex, indicating the position of available hydrological stations over the regional slope. Slope calculations were derived from a DEM constructed with SRTM data (Data available from the U.S. Geological Survey).

Wave parameters (significant height, peak wave period, wave direction and spreading) were obtained from a WatchKeeper™ buoy fitted with directional wave sensor TRIAXYS NW OEM and located in front of the estuary's inlets (Fig. 1C). This dataset is available from December 2013 – August 2015.

2.4 Evaluated scenarios

The hydrodynamics and salt transport of the Paranaguá Bay were evaluated under variable freshwater discharge and a realistic wave field using two simulations. First, a two-month simulation of the estuarine domain under variable freshwater discharge was performed to stabilize the salinity gradients. Then, a fifteen days warm-up of the wave field was performed to ensure smooth wave field propagation inside the domain. Starting from March 1st, 2015, a six-month simulation was performed, comprehending the full scale of variability on the freshwater discharge for the area (Fig. 3). This simulation included only tides and freshwater flows. A second simulation, elapsing only the month of March, was performed in which the coupled Delft3D-SWAN framework was used. March was chosen for the wave simulations due to the higher freshwater discharge in this period, so the effects of the opposing forcing conditions could be best evaluated. Wave boundary condition can be verified in the validation panel (Fig. 4 – H_s and T_p), and comprehends a variable wave field of swell and sea waves.

Four cross-sections were defined based on the limits between each subsector (Noernberg et al., 2006 - fig. 1C, thick blue lines), henceforth identified according to the sector they are in. For the cross-sections at the MZ sector, an additional N and S will be applied for the northern and southern transects, respectively (MZ_N and MZ_S). Three time periods were discerned based on the freshwater regime, and at each period a fortnightly cycle was extracted from the model data. Throughout this work time periods will be identified as FC_high, FC, FC_low and FC_waves, for periods comprehending high, mean and low freshwater discharges, and the combined high freshwater discharges and wave fields, respectively. Since the evaluated transects expand from the river mouths to the estuarine inlet, the tidal cycle was defined following the approach of Duran-Matute et al. (2014), in which a long-term mean volume is calculated for the domain of interest, and the tidal cycle is defined based on variations around this mean volume (Fig. 3). All calculations were performed considering this cycles independently.

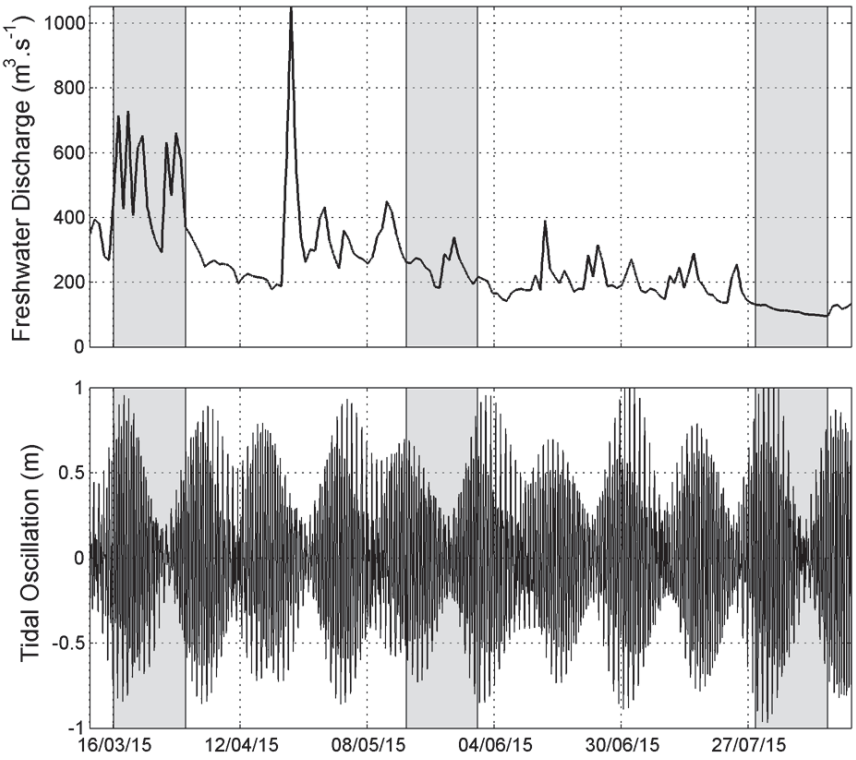

Figure 3 – Estimated total freshwater discharge for the nine drainage areas around the Paranaguá Estuarine Complex (top), and the tidal modulation defined through the volume approach (bottom) following the work of Duran-Matute et al. (2014) for the simulation period. Gray patches represent the integration periods for the fortnightly cycles.

Model quality was evaluated through the use of the root-mean square error (RMSE) and the Willmott et al. (2012) improved index of agreement (d_r). Boyle et al. (2000) points out that, although the root-mean-squared error is abundant in literature, optimizing a model only through residual variances can lead to over-fitting and significant model bias, and according to Legates and McCabe Jr (1999) the use of multiple forms of model verification ensures model robustness.

Since tidal gauge data spans several years, the period for validation of tidal elevations was based on the available current dataset, and the tidal gauge located at the PB sector was selected, since the gauge at the southern inlet was used to derive the boundary conditions. For the velocity evaluation, one month of data from a buoy-mounted ADCP (fig. 1C) was used, comprising the period from May 1st to June 1st of 2012. Fifteen stations scattered throughout the Paranaguá Bay were made available for the verification of the salinity gradients data from January and July 2013 (Martins 2013, unpublished). They correspond to vertical profiles

collected using a JFE Alec CTD, model ASTD, during the ebb phase of a spring tidal cycle. Although they do not present temporal variability they were sampled during the ebb phase of the tidal cycle, in which the highest horizontal salinity gradient is expected for the area. Every depth-averaged salinity value was compared to the closest grid node at the same time of the sampled profile. Values of the maximum salinity gradients found at each selected scenario were also compared to the ranges published by Marone et al. (2005). Wave characteristics inside the estuarine domain were validated for the chosen modeling window, from March 1st to April 1st. Since the available data for model verification did not overlap in time to each other, specific simulations were performed for all periods with spin-up runs of approximately two months beforehand.

The relative importance of tidal currents and freshwater flow in driving the hydrodynamics was evaluated using the Richardson estuarine (R_E) number (Andutta et al., 2013; Miranda et al., 2002) for each sector based on the width-averaged values of the corresponding cross-sections:

$$R_E = \frac{g\Delta\rho_H \bar{h} u_a}{\bar{\rho} u_{rms}^3} \qquad (1)$$

where g is gravity acceleration, h is the water depth, ρ is density, u_a is the residual current, $\Delta\rho_H$ is the difference in water density at each extreme of a sector, u_{rms} is the root mean square velocity, and over bars denote depth-averaged values. The flow behavior along every cross-section was evaluated based on the flow structure and long-term residual discharge (in this case, the fortnightly cycle); and salt fluxes were evaluated following the method of Hunkins (1981):

$$\frac{S}{\bar{\rho}} = u_a h_a S_a + \langle h_t u_t \rangle S_a + h_a \langle u_t S_t \rangle + h_a \bar{u}_s \bar{S}_s + h_a \langle \bar{u}' \bar{S}' \rangle + \langle u_t S_t h_t \rangle + u_a \langle S_t h_t \rangle \quad (2)$$

(a) (b) (c) (d) (e) (f) (g)

where h_a represents a mean depth, h_t depicts tidal elevations ($h_t = \eta(x,t)$), u represents the along-channel velocity component and S represents the salinity concentration. Pointy brackets (< >) represent tidal averages along the fortnightly cycle and characterizes the residual circulation (Geyer and MacCready, 2014). Subscript *a* characterizes the freshwater discharge and represents the long-term average of a property ($u_a = \langle \bar{u} \rangle$); subscript *t* characterizes the cyclical effect of tidal currents ($u_t = \bar{u} - u_a$); subscript *s* characterizes the stationary effect of the gravitational circulation ($u_s = \langle u \rangle - u_a$); and the superscript ‘ represents deviations resulting from

small-scale processes ($u' = u - u_a - u_t - u_s$). All the terms in this decomposition have an associated physical process: (a) is related to total discharge and (b) to the Stokes' drift, combined they characterize the freshwater discharge; (c) is related to tidal correlation; (d) is the gravitational circulation; (e) represents tidal pumping; (f) is associated to tidal dispersion; and (g) to residual transport influenced by wind fluctuations (Hunkins, 1981; Miranda et al., 2002).

Lastly, considering Burchard et al. (2011) evidences on the importance of tidal straining to the residual circulation in the presence of lateral advective mechanisms, which Marone et al. (2007) found in the Paranaguá Bay, all sectors were classified according to Geyer and MacCready (2014) estuarine parameter space and Hansen and Rattray (1965) stratification/circulation diagram. The former is supported on the basis of a nondimensionalization of the main forcing mechanisms, with the freshwater Froude number (Fr_f) and a mixing parameter (M) related to the effectiveness of tidal mixing, and considers the SIPS regime (Strain Induced Periodic Stratification - Simpson et al., 1990); while the latter is a more classical classification, related to the water column stratification ($\delta S/S_a$) and the relative influence of the surface currents in relation to the residual circulation (u_s/u_a). Lastly, the Simpson number (Geyer and MacCready, 2014; Simpson et al., 1990) was calculated to assess the relative importance of tidal straining under a variable freshwater discharge.

3. RESULTS

3.1 Model verification

Overall, model performance on reproducing tidal propagation and the along-shore tidal current was satisfactory, with d_r values above 0.8 (table 1, fig. 4). For the cross-shore velocities, on the hand, model performance was poor, with the model underestimating the amplitude of currents. Current velocities were decomposed into along- and cross-channel, with positive values indicating ebb currents and negative values indicating flood currents. This poor performance is most likely related to the model not properly resolving the outflows from the channel just south of the buoy location, which is only a few cells wide with the present resolution, and has a very narrow communication with the overall water body of the Paranaguá Bay. Nevertheless, even in the available data current velocities are small, and the bulk flow is related to the along-channel velocities.

Table 1 – Root mean-squared error (RMSE) and index of agreement (d_r) for the validated properties along the Paranaguá Bay. For the location of each evaluated property, see figure 1C.

	RMSE	d_r
Tidal elevations (η)	0.16 m	0.85
Along-shore velocity (U)	0.18 $m.s^{-1}$	0.80
Cross-shore velocity (V)	0.12 $m.s^{-1}$	0.39
Sig. wave height (H_s)	0.21 m	0.79
Peak wave period (T_p)	1.66 s	0.89
Salinity	2.61	0.73

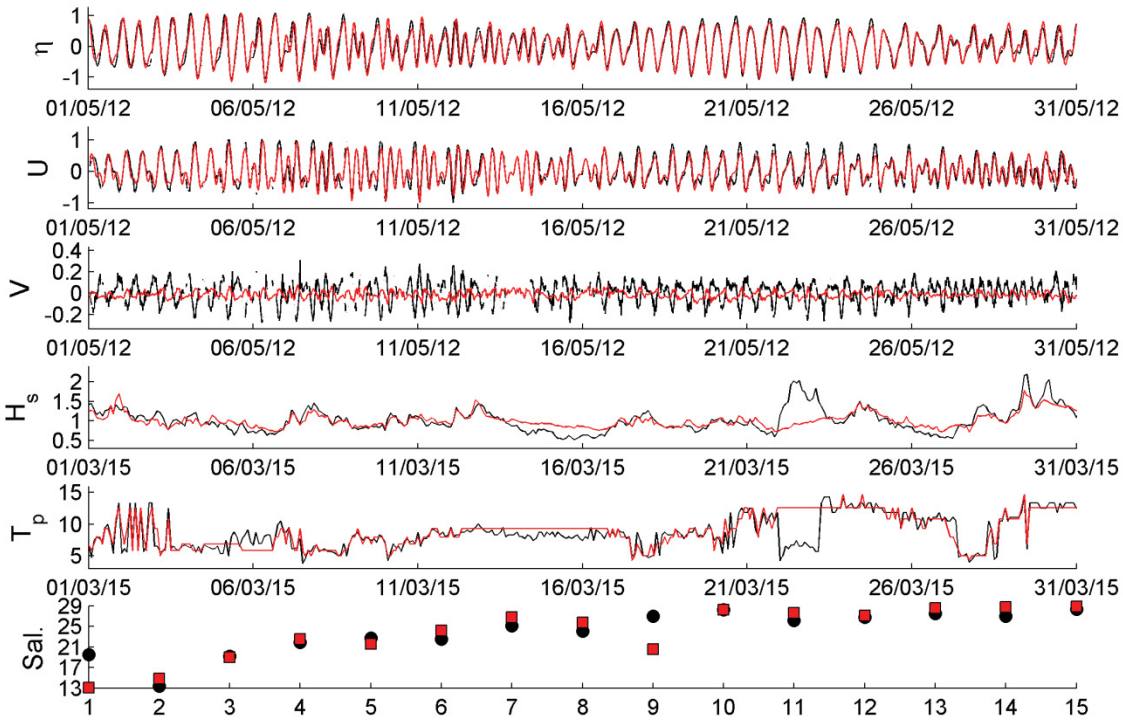

Figure 4 – Validation of model results for tidal elevations (η), along- and cross-shore current velocities (U and V, respectively), significant wave height (H_s) and peak wave period (T_p); and depth-averaged salinity concentration along the Paranaguá Bay salinity gradient. Black lines (markers) represent measured data, while red lines (marker) represent model results. For velocities, negative values represent flood currents, whereas positive values represent ebb currents. For the salinity gradient, numbers represents the stations indicate in fig. 1. Quality

indexes are presented on table 1.

The horizontal salinity gradient was well reproduced along the estuary (table 1, fig. 4), with a d_r value of 0.73. Model performance was worse at station 1 and 9, which contributed to the high value of RMSE: station 1 is located closest to the discharge point of the Cachoeira River, and has its discharged controlled by the river dam along its course; while station 9 is located closest to the Guaraguaçu River, and its discharge was estimated using the method previously outlined. The discrepancy in station 9 shows that the estimation method employed might overestimate the overall freshwater discharge in the PEC, although the overall salinity gradient along the estuary's main axis is within the available data. Calculated ranges along the main axis for the summer (wet season, 12.8 – 31.3) and the winter (dry season, 19.2 – 31.8) are within the reported values of Marone et al. (2005). The overestimation at the Guaraguaçu River is likely related to topographic gradients, as the available hydrographic stations are confined within drainage basins with higher topological gradients than the one found at the Guaraguaçu basin (fig. 2), which would naturally have lower velocities as a purely coastal plain river.

Significant wave height and peak wave period were properly reproduced, with d_r values of 0.79 and 0.88, respectively. The discrepancy that can be seen during the 22nd of March on H_s and T_p is related to a strong cold front affecting the area, with southerly winds acting for a period of three days. During this time wave direction shifted south, with increased wave height and small periods, and could not be reproduced due to a lack of wind forcing during the target simulation.

3.2 Effects of a variable boundary forcing in hydrodynamics and stratification

Overall, the Paranaguá Bay hydrodynamics is governed by tides in all sectors (table 2). R_E values range from 0.45 in the AB sector during high freshwater discharge, to as low as 0.01 in the southern inlet at the MZ sector during low discharges, indicating that even during high freshwater events tidal forces are still two times stronger than the freshwater induced circulation. At the mixture sector R_E values never exceed 0.1, and the northern inlet presents a higher influence to freshwater discharges than the southern inlet.

Table 2 – Richardson estuarine number (R_E); Simpson number (Si); Hansen and Rattray (1965) stratification and circulation parameters; and Geyer and MacCready (2014) mixing (M) and freshwater Froude number (Fr_f) parameters. Values described for all transects and time periods evaluated. For transects definition and a description of the time periods, the reader is referred to figures 1 and 3, and section 2.4 of the methods.

		R_E	Si	$\delta S/S_a$	u_S/u_a	M	Fr_f
	FC_high	0.45	0.50	0.40	6.86	1.29	1.66^{-02}
AB	FC	0.53	0.73	0.30	7.80	1.17	1.11^{-02}
Sector	FC_low	0.18	0.67	0.12	10.29	1.26	5.81^{-03}
	FC_waves	0.37	0.31	0.39	5.35	1.49	1.78^{-02}
	FC_high	0.15	0.33	0.19	7.20	1.10	1.38^{-02}
PB	FC	0.13	0.30	0.15	7.83	0.99	1.06^{-02}
Sector	FC_low	0.05	0.26	0.06	10.57	1.08	5.66^{-03}
	FC_waves	0.13	0.26	0.17	6.19	1.24	1.33^{-02}
	FC_high	0.09	0.22	0.13	3.65	1.16	2.45^{-02}
MZ_N	FC	0.08	0.21	0.11	4.19	1.06	1.91^{-02}
Sector	FC_low	0.03	0.14	0.04	3.49	1.22	1.45^{-02}
	FC_waves	0.07	0.18	0.10	3.63	1.28	2.29^{-02}
	FC_high	0.04	0.2	0.08	10.99	1.11	7.54^{-03}
MZ_S	FC	0.06	0.19	0.07	8.66	1.01	9.66^{-03}
Sector	FC_low	0.01	0.13	0.03	15.13	1.13	2.78^{-03}
	FC_waves	0.05	0.14	0.08	7.22	1.28	1.25^{-02}

Residual discharges calculated for all cross-sections show an increasing export of water from dry to rainy season according to the increase in freshwater discharge for all river only cases, as expected. In the case of the combined high freshwater discharge and waves, however, discharge values are reduced to levels similar to the ones during mean runoff rates (fig. 5). These results would suggest a considerable effect of the wave forcing on the overall hydrodynamics of the Paranaguá Bay, but only very small waves (under 0.5 m) are capable of

entering the PEC through both of its inlets (fig. 6). This leads to only small differences on the R_E values under the effect of combined freshwater flow and waves, and in the stratification in all sectors according to the Hansen and Rattray (1965) stratification parameter and the Simpson number (table 2).

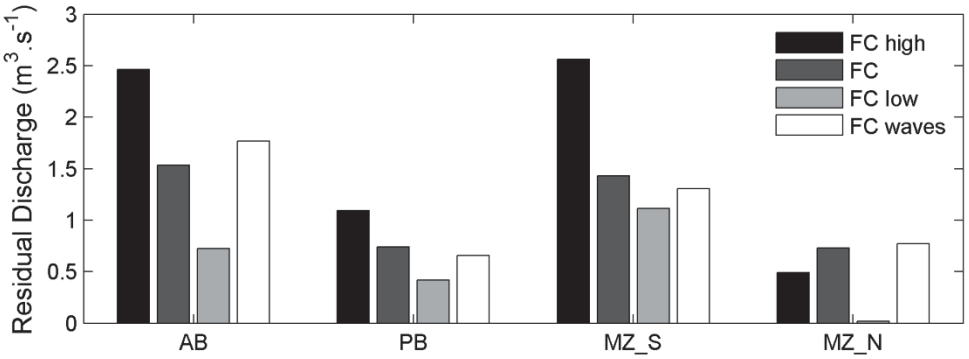

Figure 5 – Residual discharge (in $m^3.s^{-1}$) for a fortnightly cycle along cross-sections at each of the three sectors: the Antonina bay (AB), the Paranaguá bay (PB) and the mixture zone north (MZ_N) and south (MZ_S) transects. Positive values represent ebb directed flows whereas negative values represent flood flows. Freshwater discharge rates are separated according to the chosen periods, and identified in figure 3 and section 2.4.

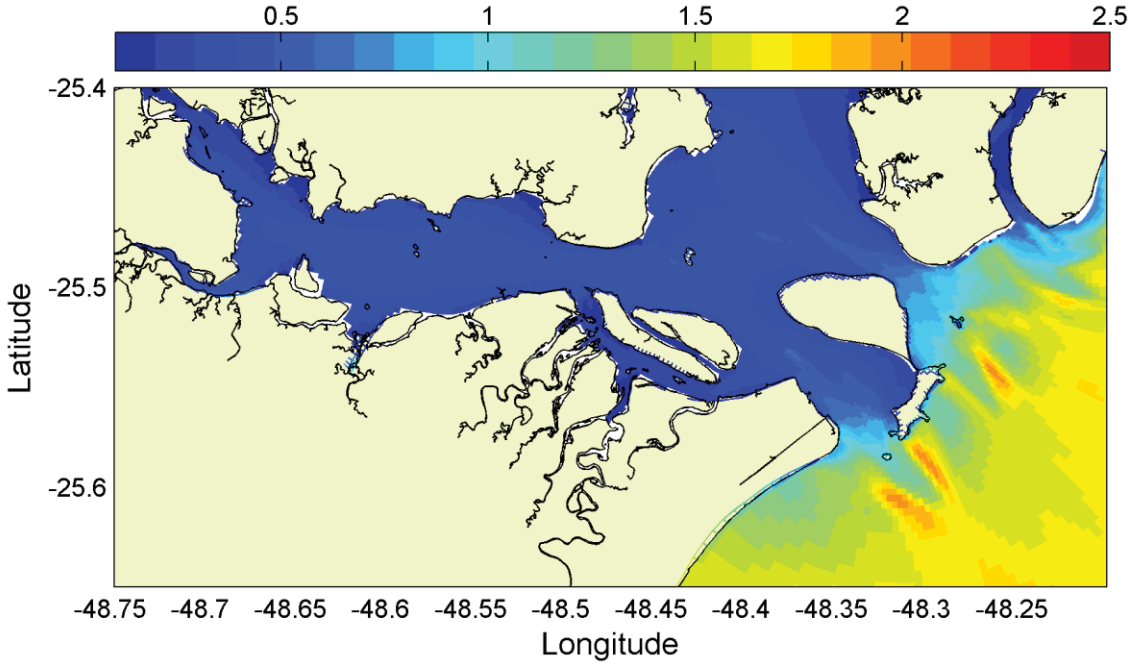

Figure 6 – Maximum simulated significant wave height (H_s) inside the Paranaguá Bay for the

FC_waves time period.

Regardless of freshwater discharge rates or the presence of a wave forcing, the spatial structure of the depth-averaged residual circulation (fig. 7) is not affected, only its magnitude, with maximum values of 0.4 $m.s^{-1}$ at the inlets on the mixture sector. In the AB sector ebb-directed residuals dominate from both river outlets, with flood directed flows restricted to the navigational channel and the margins of shallow banks. Entering in the PB sector a duality between ebb and flood ensues, with the northern margin mainly dominated by ebb flows, and the south margin by the flood flows. For both sectors, eddy motion tends to persist around shallower banks and in the interface between the two dominant flows. In the mixture zone a more complicated pattern can be discerned, with water from the N-S axis and the E-W axis (Paranaguá Bay) converging. In this sector water inflow tends to dominate the middle portions of the cross-sections, while ebb flows dominate the flanks and a large eddy develops behind Mel Island. At the southern inlet, flood dominates the shallow bank known as “Saco do Limoeiro”, and the ebb is pushed towards the navigational channel and the southwest margin. The presence of a rocky outcrop (Galheta Island) at the southern inlet, combined with the higher depths (up to 35 m) of the navigational channel (fig. 1), produces a hydraulic jetty between the Galheta and Mel islands which can be seen on the residual currents.

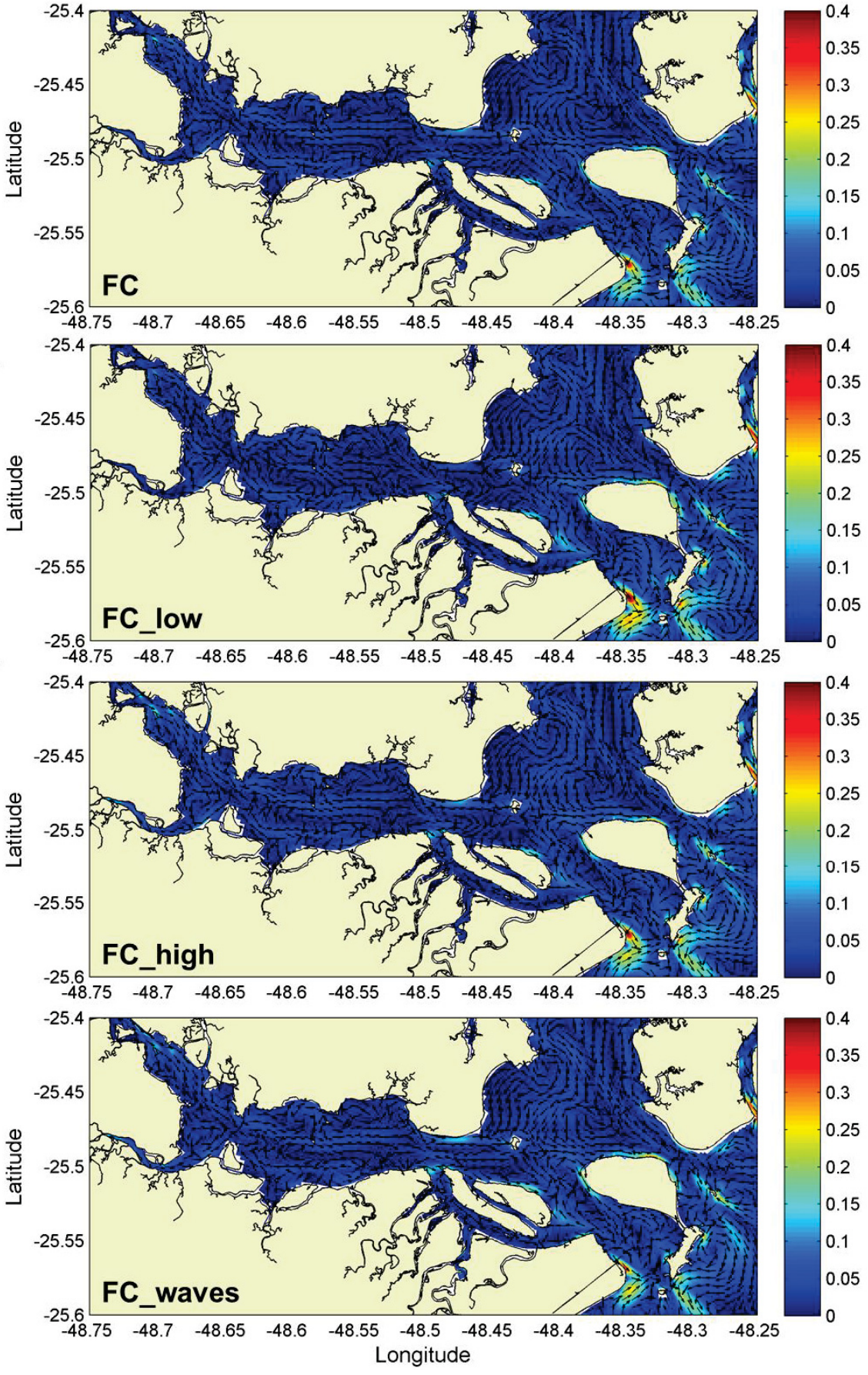
FC
FC_low
FC_high
FC_waves
Latitude
Longitude
-25.4
-25.45
-25.5
-25.55
-25.6
-48.75
-48.7
-48.65
-48.6
-48.55
-48.5
-48.45
-48.4
-48.35
-48.3
-48.25
0.4
0.35
0.3
0.25
0.2
0.15
0.1
0.05
0

Figure 7 – Residual circulation magnitude (m.s^{-1} - color scale) and direction (arrows) for all evaluated periods. For a description of the scenarios, the reader is referred to figure 3 and section 2.4 of the methods.

This stability on the horizontal spatial structure of the residual circulation is reflected on the vertical profiles. The flow structure at every cross-section was evaluated, and despite the expected differences on the magnitude of the residual circulation, the flow pattern present only slight variations. Figure 8 compares the vertical flow structure for the highest and lowest freshwater discharge scenarios. Overall, flood dominates the deepest channels whereas ebb dominates the shallower margins and the upper layers of the cross-section. During increased river runoff a higher portion of the water column is dominated by the ebb flows, represented by the displacement of the 0.05 m.s^{-1} contour line, and the flood currents are compressed closer to the waterbed.

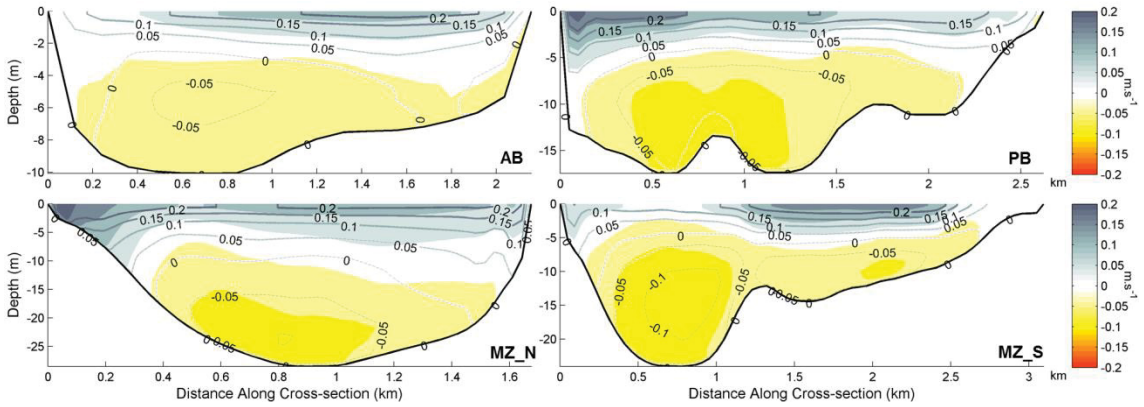

Figure 8 – Depth-dependent residual velocities (in m.s^{-1}) at the evaluated cross-sections. Patches represent current values during the low freshwater scenarios, whereas contours represent currents during high freshwater flows. Magnitude is matched between the color scale, contours and patches, with positive values indicating ebb discharges, and negative values indicating flood discharges. For the location of every cross-section, the reader is referred to figure 1.

Combining the effects of tidal circulation, freshwater induced flows and stratification (table 2), the sectors along Paranaguá Bay are classified following the classical method of

Hansen and Rattray (1965) and the novel approach of Geyer and MacCready (2014). H&R classifies the Paranaguá Bay, with the exception of the southern inlet, as type 2b during mid to high freshwater discharge scenarios, and type 2a for low freshwater discharges periods. The southern inlet is classified as type 2a across all conditions. This indicates partially mixed conditions during all scenarios with a predominant upstream transport of salt, and shows that turbulence in the southern inlet is more effective in mixing the water column. Geyer and MacCready (2014) freshwater Froude number and mixing parameter approach classifies all sectors of the Paranaguá Bay under the SIPS regime, indicating that stratification can persist throughout the tidal cycle with well-mixed conditions during the flood stage of tides. Simpson's number for all sectors are below the 0.8 limit, indicating that permanently stratified conditions are not reached in any sector (Becherer et al., 2011).

3.3 Consequences on the advective salt flux

The advective salt flux (ASF) was calculated with equation (1) for all stations on each cross-section, and all terms were then averaged over the section width. Since most cross-sections are inhomogeneous, both the obtained mean value and the standard deviation is presented (table 3). Although Hunkins (1981) methodology is not indicated for this type of cross-sections, the sign on each term is still significant to determine the related physical processes relative contribution to dispersion or advection of salt.

For all cross-sections and all time periods, terms (f) and (g) - related to oscillatory dispersion, were at least two orders of magnitude smaller than the smallest term (term (e)), and are therefore ignored on the analyses. The freshwater discharge was the only term responsible for removing salt from the estuary, with the exception of the southern inlet. In this inlet, the high dispersive behavior of the southwest margin surpassed the advective effects on the rest of the cross-section, generating a dispersive total discharge. This can be seen by the small mean values on the freshwater term with high standard deviations, and by the spatial variation on its values (fig. 9). Tidal correlation, gravitational circulation and tidal pumping all acted as dispersive mechanisms across all section and time periods, the latter being the least effective. Gravitational circulation dominated the inner sectors of the Paranaguá Bay (AB and PB sectors), while tidal correlation was the dominant term in the mixture zone. Like for the spatial

structure of the flow, only differences in the amplitude of the mechanisms were verified between different time periods.

Table 3 – Advective salt flux (in $kg.m^{-1}.s^{-1}$) according to equation (1), for the processes of freshwater discharge (terms a + b), tidal correlation (term c), gravitational circulation (term d) and tidal pumping (term e). Negative values indicate dispersion mechanisms, while positive values indicate advection of salt. Values were width-averaged along each cross-section, and the mean values ± the standard deviation is given. For a definition of sectors and time periods, the reader is referred to section figure 1 and 3, and section 2.4 of this work.

		Freshwater Discharge	Tidal Correlation	Gravitational Circulation	Tidal Pumping	∑(a-g)
AB Sector	FC_high	3.54 ± 4.15	-0.94 ± 1.17	-1.25 ± 0.52	-0.26 ± 0.09	1.14 ± 5.48
	FC	2.59 ± 4.57	-0.67 ± 0.84	-0.86 ± 0.35	-0.17 ± 0.06	0.92 ± 5.47
	FC_low	1.26 ± 3.09	-0.31 ± 0.4	-0.27 ± 0.17	-0.1 ± 0.05	0.6 ± 3.56
	FC_waves	2.64 ± 3.58	-0.81 ± 1.15	-0.87 ± 0.41	-0.22 ± 0.09	0.79 ± 4.84
PB Sector	FC_high	5.4 ± 10.17	-0.57 ± 1.46	-1.59 ± 0.7	-0.18 ± 0.13	3.09 ± 11.77
	FC	3.88 ± 9.8	-0.39 ± 0.88	-1.14 ± 0.49	-0.16 ± 0.09	2.21 ± 10.79
	FC_low	2.45 ± 8.69	-0.21 ± 0.72	-0.42 ± 0.26	-0.09 ± 0.05	1.75 ± 9.48
	FC_waves	3.79 ± 11.95	-0.59 ± 1.52	-1.11 ± 0.61	-0.13 ± 0.08	2.0 ± 13.55
MZ_N Sector	FC_high	16.27 ± 18	-2.23 ± 1.49	-1.73 ± 0.96	-0.49 ± 0.21	11.83 ± 20.1
	FC	9.37 ± 23.05	-1.48 ± 1.06	-1.46 ± 0.87	-0.35 ± 0.15	6.11 ± 24.75
	FC_low	7.29 ± 13.59	-0.71 ± 0.74	-0.36 ± 0.25	-0.2 ± 0.1	6.02 ± 14.46
	FC_waves	7.94 ± 18.21	-1.7 ± 1.24	-1.17 ± 0.79	-0.34 ± 0.16	4.75 ± 20.06
MZ_S Sector	FC_high	-0.63 ± 18.6	-0.86 ± 1.46	-0.91 ± 0.6	-0.31 ± 0.21	-2.7 ± 19.94
	FC	1.0 ± 18.63	-0.52 ± 1.25	-0.84 ± 0.55	-0.22 ± 0.13	-0.57 ± 19.82
	FC_low	-3.03 ± 17.23	-0.41 ± 0.97	-0.22 ± 0.15	-0.14 ± 0.09	-3.8 ± 17.65
	FC_waves	0.67 ± 18.97	-1.04 ± 1.6	-0.74 ± 0.53	-0.31 ± 0.2	-1.41 ± 20.44

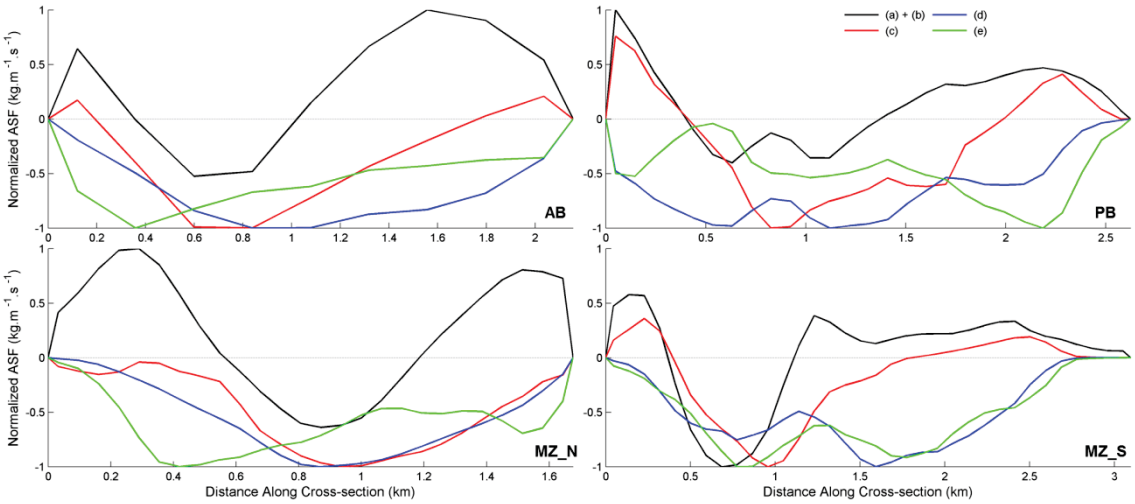

Figure 9 – Advective salt flux (ASF – $kg.m^{-1}.s^{-1}$) normalized by its maximum value at each cross-section for the FC time period. Only the terms representing the freshwater discharge (terms (a) + (b)), tidal correlation (term (c)), gravitational circulation (term (d)) and tidal pumping (term (e)) are displayed. Positive values represent advective salt fluxes, while negative values represent dispersive salt fluxes.

4. DISCUSSION AND CONCLUSIONS

Although the proposed estimation for the freshwater discharge surrounding the Paranaguá Estuarine Complex showed some disagreement with measured salinity gradients outside the Guaraguaçu River (drainage basin I – fig. 2), the salinity gradient along the Paranaguá Bay was well represented. Using this estimation, the long-term average freshwater discharge for the year of 2015 would be of about 250 $m^3.s^{-1}$, close to the average estimation made by Marone et al. (2005). The model was also able to reproduce well the main current component of the circulation, and the disagreement on the cross-shore component is most likely related to poor definition of the Cotinga Channel. A refined domain of this channel would be required to properly represent its outflows, which is not feasible with the current domain configuration and it is not the goal of this work. Model results showed the same pattern of higher ebb currents over flood currents described by several authors along different portions of the Paranaguá Bay (Lana et al., 2001; Mantovanelli et al., 2004; Noernberg et al., 2007), and tidal asymmetry was well reproduced, with longer floods and shorter ebbs and events of double high and low water, the latter specially during neap tides (Lana et al., 2001; Marone and Jamiyanaa, 1997). At the PEC's inlets, Angulo (1999) described a two-channel morphology for the northern

inlet, a large ebb tidal delta at the southern inlet, and a flood tidal delta at Saco do Limoeiro. All these features can be recognized on the depth-averaged residual circulation (fig. 7).

At every evaluated cross-section, residual discharges indicated an increasing export of water from dry to rainy conditions. Although this increase affected the magnitude of the residual circulation, it did not affect its pattern. This is mainly attributed to the higher influence of tidal forces in driving the hydrodynamics, as indicated by the R_E values. The riverine discharge itself does not appear to play a significant role in governing the hydrodynamics, but the horizontal salinity gradient due to the river-tidal interaction produces buoyancy fluxes that drive an up-estuary bottom flow and a down-estuary surface flow. This pattern can be identified in all cross-sections (fig. 8) and is defined as the exchange flow or the estuarine circulation (Geyer and MacCready, 2014; MacCready and Geyer, 2010). Fischer (1972) pointed out that in wide estuaries the estuarine circulation could happen in the lateral dimension due to the development of lateral baroclinic gradients forced by variations in depth. This would lead to down-estuary transport in the shallower flanks and up-estuary transport in the deeper channels, which seems to be the case along the PB sector and some portions of the mixture zone (Fig. 7). This type of circulation affects the dispersion of pollutants/dissolved matter depending on their vertical position in the water column, and can greatly augment the longitudinal dispersion of passive tracers (Geyer and MacCready, 2014). This can be important along the seasonal cycle for the Paranaguá Bay, as it has been shown that the seasonal scale affects the concentration of dissolved nutrients and biological productivity in the water column (Lana et al., 2001; Mizerkowski et al., 2012); and at the interface between the sectors PB and AB, where Noernberg (2001) found a high turbidity zone at the navigational channel. He first hypothesized that this area could be considered an ETM (Estuarine Turbidity Maximum) zone, but this increased suspended particulate matter concentration is most likely a result of the confluence between the outflowing discharges of the AB sector and the inflowing water following the navigational channel at the PB sector (fig. 7 and 8). This would be unrelated to the classical notion of an ETM, which is the result of the energy balance between tidal forces and freshwater discharges at the tip of the salt wedge (Dyer, 1995), and more related to the turbulence generated by the conflicting flow directions and the strong inflow of bottom currents that trap sinking particles (Traykovski et al., 2004).

Wave action inside the estuary was limited (fig. 6), but produced an overall decrease in the circulation magnitude inside the PEC (fig. 5). Luo et al. (2013) encountered a similar pattern in the Mersey estuary simulating wave action over the Liverpool Bay. In both cases, the presence of sand banks and deltas sheltered the estuary from incoming wave energy. Based on these findings, the Galheta's Bank shallow depths (< 5 m) compared to the surrounding regions act as the main energy dissipation mechanism for the southern inlet, whereas at the northern inlet it is a consequence of the combination of the bars and sand banks described by Angulo (1999) around Palmas island. Bolaños et al. (2014) studied the wave effects on the residual circulation for the Dee estuary, in Liverpool Bay. These authors found that, for a wide-mouth estuary, waves had little impact on circulation, and the increased ebb surface flows due to the gravitational circulation acted to damp wave intrusion. A similar effect was verified at the PEC, with waves having little impact on the bay's circulation and acting more as an "energy fence" to the estuarine discharge. Even at the northern inlet, where Angulo (1999) identified a higher susceptibility to wave action, the spatial structure of the flow did not present significant changes. Regardless of the forcing conditions, the northern inlet presented a higher equilibrium state – especially noticeable during low freshwater discharges. The dominance of ebb discharges at the southern inlet is probably related to the dredging of the navigational channel in the area, creating a preferential pathway for tidal currents as identified by Noernberg et al. (2007).

This horizontal and vertically bi-directional flow along the Paranaguá Bay governed the advective salt fluxes. The freshwater discharge is the only process to consistently remove salt from the bay, especially through the upper layers of the water column. This tendency is only deviated from at the southern inlet. In this cross-section removal and intake of salt occurs mostly due to the horizontal bathymetric gradient. This illustrates the process described by Fischer (1972) and its influenced by the combination of flows coming from the PB sector and towards the Cotinga channel, the latter having shown a flood tendency even during high freshwater discharges. Gravitational circulation and tidal correlation are the major dispersive mechanisms, with their relative importance changing depending on the evaluated sector and time period. Gravitational circulation is dependent on the steady shear dispersion related to tidal mixing and freshwater discharge (Lerczak et al., 2006), so it is expected to respond to variations in the exchange flow, and is the dominant dispersive mechanism for most time periods.

Maximum values along the cross-section were found at the deepest channels (fig. 9), where vertical stratification is highest. Tidal correlation is related to topographic trapping of water during a tidal stage with subsequent release at a later time, which is normally associated with complex bathymetries and shallow areas, *e.g.* mudflats (Fischer et al., 1979). It dominated salt dispersion during low freshwater periods, and its maximum value along the cross-section (fig. 9) were found in areas with a changing bathymetry or opposing flow dominances, e.g. at the PB and MZ_S cross-sections. The ratio between the water body and tidal flats is between 15% to 30% from the inlets to the AB sector (Noernberg et al., 2006), and showed an overall flood dominance over shallow banks (fig. 7). This indicates the importance of better understanding the hydrodynamics over these areas to better determine the salt fluxes in the Paranaguá Bay. This process also dominates salt dispersion for all time periods at the northern inlet cross-section, likely associated to the non-local advective salt fluxes described by Dronkers and van de Kreeke (1986). Tidal pumping contributes the least to the dispersion of salt during the evaluated scenarios, regardless of freshwater input. Fischer et al. (1979) relates this process to the straining of the salinity fields due to the vertical shear of the tidal current, which agrees to the results found herein, as maximum values were found at the interface between flood and ebb dominated stations along the cross-section where this shear is expected to be greater.

Both estuarine classifications employed for the Paranaguá Bay sectors shows the importance of stratification to the bay dynamics. Although the partially-mixed nature of the Paranaguá Bay was previously reported by Knoppers et al. (1987), the use of Geyer and MacCready's (2014) mixing parameter and freshwater Froude number classifies all sectors into the SIPS regime. This classification gives more insight into the building and breaking of stratification along the tidal cycle, as it indicates that full water column mixing can occur during the flood stages of tides, while a more stable water column is found during the ebb. These transitions can be verified with the Simpson number (table 2, Simpson et al., 1990). Stacey and Ralston (2005) found that for $Si < 0.2$ well-mixed conditions are expected along the complete tidal cycle, whereas the SIPS regime starts to occur for $Si > 0.2$. This indicates that the northern and southern inlet cross-section can be well mixed throughout the tidal cycle for periods with low discharges, but vertical stratification is expected for all cross-sections under higher freshwater periods. Waves, in this instance, promote increased vertical mixing at the mixture

zone, and reduce Si values for the area, indicating that even during high freshwater events the estuarine inlets can present well-mixed conditions due to wave action.

In summary, a 3-D model of the Paranaguá Estuarine Complex (PEC) was used to evaluate the effects of seasonal variations in freshwater discharge and a realistic wave field on the hydrodynamics and advective salt transport of the Paranaguá Bay. Although freshwater discharge shows a steep variation along the seasonal scale, tidal forces are at least twice more important in determining the hydrodynamics of the Paranaguá Bay. Wave action will mainly act as an energy fence to the estuarine outflow, reducing its magnitudes and increasing mixing in the inner region close to the estuarine inlets, but will not alter the circulations patterns inside the bay. These waves will have only a small impact on the advective salt fluxes along Paranaguá Bay, with the freshwater discharge acting to remove salt while the gravitational circulation and tidal correlation acts as the main dispersive mechanisms. Although previously classified as a partially-mixed system, Geyer and MacCready's (2014) classification characterizes the Paranaguá Bay under the SIPS regime. This indicates a higher capacity of tides to mix the water column during the flood stages of tides, producing a periodic stratification, and give new insights regarding the stratification processes along Paranaguá Bay.

Acknowledgements

The authors would like to thank Dr. César de Castro Martins for the salinity data; the Paranaguá Pilots and the APPA-CEM partnership for the ADCP and tidal gauge datasets along Paranaguá Bay. M. M. Souza would like to thank CAPES (Coordenação de Aperfeiçoamento de Pessoal do Ensino Superior) for the MSc. Scholarship. This study is a contribution from INCT-Mar COI (CNPq, Proc. 565062/2010-7).

REFERENCES

Andutta, F.P., Miranda, L.B. de, Schettini, C.A.F., Siegle, E., Silva, M.P. da, Izumi, V.M., Chagas, F.M., 2013. Temporal variations of temperature , salinity and circulation in the Peruípe river estuary (nova Viçosa , BA). Cont. Shelf Res. 70, 36–45. doi:10.1016/j.csr.2013.03.013

Angulo, R.J., 1999. Morphological Characterization of the Tidal Deltas on the Coast of the State of Paraná. An. Acad. Bras. Cienc. 71, 935–959.

Becherer, J., Burchard, H., Flöser, G., Mohrholz, V., Umlauf, L., 2011. Evidence of tidal straining in well-mixed channel flow from micro-structure observations. Geophys. Res. Lett. 38, 2–6. doi:10.1029/2011GL049005

Bolaños, R., Brown, J.M., Souza, A.J., 2014. Wave–current interactions in a tide dominated estuary. Cont. Shelf Res. 87, 109–123. doi:10.1016/j.csr.2014.05.009

Booji, N., Ris, R.C., Holthuijsen, L.H., 1999. A third generation wave model for coastal regions, Part I, Model description and validation. J. Geophys. Res. 104, 7649–7666.

Boyle, D.P., Gupta, H. V, Sorooshian, S., 2000. Toward Improved Calibration of Hydrologic Models: Combining the Strengths of Manual and Automatic Methods. Water Resour. Res. 36, 3663–3674. doi:10.1029/2000WR900207

Burchard, H., Hetland, R.D., Schulz, E., Schuttelaars, H.M., 2011. Drivers of Residual Estuarine Circulation in Tidally Energetic Estuaries: Straight and Irrotational Channels with Parabolic Cross Section. J. Phys. Oceanogr. 41, 548–570. doi:10.1175/2010JPO4453.1

Dronkers, J., van de Kreeke, J., 1986. Experimental determination of salt intrusion mechanisms in the Volkerak estuary. Netherlands J. Sea Res. 20, 1–19. doi:10.1016/0077-7579(86)90056-6

Duran-Matute, M., Gerkema, T., de Boer, G.J., Nauw, J.J., Gräwe, U., 2014. Residual circulation and freshwater transport in the Dutch Wadden Sea: a numerical modelling study. Ocean Sci. 10, 611–632. doi:10.5194/os-10-611-2014

Dyer, K.R., 1995. Sediment transport processes in estuaries, in: Perillo, G.M.E. (Ed.), Geomorphology and Sedimentology of Estuaries. Elsevier Science B. V., pp. 423–449.

Elias, E.P.L., Hansen, J.E., 2013. Understanding processes controlling sediment transports at the mouth of a highly energetic inlet system (San Francisco Bay, CA). Mar. Geol. 345, 207–220. doi:10.1016/j.margeo.2012.07.003

Fischer, H., 1972. Mass transport mechanisms in partially stratified estuaries. J. Fluid Mech. 53, 671. doi:10.1017/S0022112072000412

Fischer, H.B., List, E.J., Koh, R.C.Y., Imberger, J., Brooks, N.H., 1979. Mixing in Inland and Coastal Waters. Academic Press, New York.

Geyer, W.R., MacCready, P., 2014. The Estuarine Circulation. Annu. Rev. Fluid Mech. 46, 175–197. doi:10.1146/annurev-fluid-010313-141302

Hansen, D. V, Rattray Jr., M., 1965. Gravitational circulation in straits and estuaries. J. Mar. Res. 23, 104–122.

Hu, K., Ding, P., Wang, Z., Yang, S., 2009. A 2D/3D hydrodynamic and sediment transport model for the Yangtze Estuary, China. J. Mar. Syst. 77, 114–136.

Hunkins, K., 1981. Salt Dispersion in the Hudson Estuary. J. Phys. Oceanogr. 11, 729–738.

Kjerfve, B., 1989. Estuarine geomorphology and physical oceanography, in: Day Jr., J.W., Hall, C.A.S., Kemp, W.M., Yáñez-Arancibia, A. (Eds.), Estuarine Ecology. John Wiley & Sons, Inc., pp. 47–78.

Knoppers, B.A., Brandini, F.P., Thamm, C.A., 1987. Ecological studies in the Bay of Paranaguá. II. Some physical and chemical characteristics. Nerítica 2, 1–36.

Lamour, M.R., Soares, C.R., Carrilho, J.C., 2004. Mapas de parâmetros texturais de sedimentos de fundo no Complexo Estuarino de Paranaguá – PR. Bol. Parana. Geociências 55, 77–82.

Lana, P.C., Marone, E., Lopes, R.M., Machado, E.C., 2001. The subtropical Estuarine Complex of Paranaguá Bay, Brazil, in: Seeliger, U., Kjerfve, B. (Eds.), Coastal Marine Ecosystems of Latin America. Ecological Studies, pp. 131–145.

Legates, D.R., McCabe Jr, G.J., 1999. Evaluating the use of “goodness-of-fit” measures in hydrologic and hydroclimatic model validation. Water Resour. Res. 35, 233–241.

Lerczak, J.A., Geyer, W.R., 2004. Modeling the Lateral Circulation in Straight, Stratified Estuaries*. J. Phys. Oceanogr. 34, 1410–1428. doi:10.1175/1520-0485(2004)034<1410:MTLCIS>2.0.CO;2

Lerczak, J.A., Geyer, W.R., Chant, R.J., 2006. Mechanisms Driving the Time-Dependent Salt Flux in a Partially Stratified Estuary*. J. Phys. Oceanogr. 36, 2296–2311. doi:10.1175/JPO2959.1

Lesser, G.R., Roelvink, J. a., van Kester, J. a. T.M., Stelling, G.S., 2004. Development and validation of a three-dimensional morphological model. Coast. Eng. 51, 883–915. doi:10.1016/j.coastaleng.2004.07.014

Luo, J., Li, M., Sun, Z., O’Connor, B.A., 2013. Numerical modelling of hydrodynamics and sand

transport in the tide-dominated coastal-to-estuarine region. Mar. Geol.

MacCready, P., 2011. Calculating Estuarine Exchange Flow Using Isohaline Coordinates. J. Phys. Oceanogr. 41, 1116–1124. doi:10.1175/2011JPO4517.1

MacCready, P., Geyer, W.R., 2010. Advances in estuarine physics. Ann. Rev. Mar. Sci. 2, 35–58. doi:10.1146/annurev-marine-120308-081015

Mantovanelli, A., Marone, E., da Silva, E.T., Lautert, L.F., Klingenfuss, M.S., Prata, V.P., Noernberg, M.A., Knoppers, B.A., Angulo, R.. J., 2004. Combined tidal velocity and duration asymmetries as a determinant of water transport and residual flow in Paranaguá Bay estuary. Estuar. Coast. Shelf Sci. 59, 523–537. doi:10.1016/j.ecss.2003.09.001

Marone, E., Jamiyanaa, D., 1997. Tidal characteristics and a numerical model for the M2 tide at the Estuarine Complex of the Bay of Paranaguá, Paraná, Brazil. Nerítica 11, 95–107.

Marone, E., Machado, E.C., Lopes, R.M., Silva, E.T. da, 2005. Land-ocean fluxes in the Paranaguá Bay estuarine system, southern Brazil. Brazilian J. Oceanogr. 53, 169–181. doi:10.1590/S1679-87592005000200007

Marone, E., Noernberg, M.A., Lautert, L.F., dos Santos, I., Fill, H.D., Buba, H., Marenda, A., 2007. Medições de correntes e curva vazão-maré na Baía de Paranaguá, PR. Bol. Parana. Geociências 60-61, 55–64.

Martins, G.J., Marone, E., Angulo, R.J., Noernberg, M.A., Quadros, C.J.L. de, 2004. Dinâmica da zona rasa de shoaling e o transporte de sedimentos na desembocadura sul do Complexo Estuarino de Paranaguá - PR. Bol. Parana. Geociências 54, 51–64.

Mayerle, R., Narayanan, R., Etri, T., Wahab, A.K.A., 2015. A case study of sediment transport in the Paranagua Estuary Complex in Brazil. Ocean Eng. 106, 161–174. doi:10.1016/j.oceaneng.2015.06.025

Miranda, L.B. de, Castro, B.M. de, Kjerfve, B., 2002. Princípios de Oceanografia Física de Estuários. Editora da Universidade de São Paulo, São Paulo, Brazil.

Miranda, L.B. De, Olle, E.D., Bérgamo, A.L., Silva, S., Andutta, F.P., Oceanográfico, P., Paulo, S., Tecnologia, F. De, Lara, R., Gusmão, A.B. De, 2012. CIRCULATION AND SALT INTRUSION IN THE PIAÇAGUERA CHANNEL , SANTOS (SP) Universidade Federal do Pará 60, 11–23.

Mizerkowski, B.D., Hesse, K.-J., Ladwig, N., Machado, E. da C., Rosa, R., Araujo, T., Koch, D.,

2012. Sources, loads and dispersion of dissolved inorganic nutrients in Paranaguá Bay. Ocean Dyn. doi:10.1007/s10236-012-0569-x

Nemes, D.D., Marone, E., 2013. Caracterização das ondas de superfície na plataforma interna do Estado do Paraná , Brasil. Bol. Parana. Geociências 68, 12–25.

Noernberg, M. de A., Marone, E., Angulo, R.J., 2007. Coastal currents and sediment transport in Paranaguá Estuary Complex Navigation Channel. Bol. Parana. Geociências 60-61, 45–54.

Noernberg, M.A., 2001. Processos Morfodinâmicos no Complexo Eestuarino de Paranaguá – Paraná - Brasil : um estudo a partir de dados in situ e LANDSAT-TM. Universidade Federal do Paraná.

Noernberg, M.A., Lautert, L.F.C., Araújo, A.D., Marone, E., Angelotti, R., Netto Jr., J.P.B., Krug, L.A., 2006. Remote Sensing and GIS Integration for Modelling the Paranaguá Estuarine Complex -Brazil. J. Coast. Res. 39, 1627–1631.

Simpson, J.H., Brown, J., Matthews, J., Allen, G., 1990. Tidal Straining, Density Currents, and Stirring in the Control of Estuarine Stratification. Estuaries 13, 125. doi:10.2307/1351581

Soares, C.R., Lamour, M.R., 2008. A “Barra de Paranaguá” e a evolução batimétrica do delta de maré vazante na desembocadura do Complexo Estuarino de Paranaguá (PR), in: Boldrini, E.B., Soares, C.R., de Paula, E. V (Eds.), Dragagens Portuárias No Brasil: Engenharia, Tecnologia E Meio Ambiente. Associação de Defesa do Meio Ambiente e Desenvolvimento de Antonina (ADEMADAN), Faculdades Integradas Espírita (UNIBEM), e Secretaria de Ciência e Tecnologia para Inclusão Social (MCT), Antonina, pp. 69–87.

Stacey, M.T., Ralston, D.K., 2005. The Scaling and Structure of the Estuarine Bottom Boundary Layer. J. Phys. Oceanogr. 35, 55–71.

Traykovski, P., Geyer, R., Sommerfield, C., 2004. Rapid sediment deposition and fine-scale strata formation in the Hudson estuary. J. Geophys. Res. 109, 1–20. doi:10.1029/2003JF000096

Willmott, C.J., Robeson, S.M., Matsuura, K., 2012. A refined index of model performance. Int. J. Climatol. 32, 2088–2094. doi:10.1002/joc.2419

WL|DelftHydraulics, 2006. Delft3D-FLOW User Manual.